



Preparation of γ -Al₂O₃/ α -Al₂O₃ ceramic foams as catalyst carriers via the replica technique

Vladimir Shumilov^a, Alexey Kirilin^a, Anton Tokarev^a, Stephan Boden^b, Markus Schubert^b, Uwe Hampel^b, Leena Hupa^a, Tapio Salmi^a, Dmitry Yu. Murzin^{a,*}

^a Johan Gadolin Process Chemistry Centre, Abo Akademi University, FI-20500 Turku/Abo, Finland

^b Institute of Fluid Dynamics, Helmholtz-Zentrum Dresden-Rossendorf, Bautzner Landstr. 400, 01328 Dresden, Germany

ARTICLE INFO

Keywords:

γ -Al₂O₃/ α -Al₂O₃

Catalytic foams

Macroporous ceramics

Hydrogenation of ethylbenzoylformate

ABSTRACT

This work describes an effective method for the preparation of open-cell ceramic foams for their further use as catalyst supports. The polyurethane sponge replica technique was applied using a ceramic suspension based on a mixture of α -alumina, magnesia and titania and polyvinyl alcohol solution as a liquid component. The polyurethane sponge was etched with NaOH and covered with colloidal silica to obtain better adhesion of the slurry to the walls of the polymeric material onto it. The surface area of the ceramic carrier was increased by adding a layer of γ -alumina. Deposition of an active catalytic phase (Pt) was done by impregnation. Properties of the carriers and the final catalyst were investigated by a number of physico-chemical methods such as TEM, SEM, XRD and computer tomography. Hydrogenation of ethyl benzoylformate was performed to elucidate the catalytic properties of foam catalysts illustrating their applicability.

1. Introduction

One of the current important topics in catalytic reaction engineering is the optimization and intensification of catalytic reactors with the aid of advanced structured materials. For three phase processes structural packing are used to enhance the gas-liquid-solid contact area and turbulence within the fluid phase, thus increasing the interfacial mass transfer. It has been demonstrated for two- phase and three-phase reactions that structured packings, e.g. open cell foams, have better hydrodynamic performance than conventional packings such as for example Raschig rings [1]. Cellular structures perform remarkably well in continuous liquid- phase catalytic processes giving a low pressure drop and enhanced mass transfer [2].

Macroporous ceramic foams are porous, lightweight, solid materials with high density, large specific surface area, high thermal stability and resistance to chemical attacks [3,4]. Ceramic foams consist of cellular structures composed of three-dimensional networks of struts [5].

The common types of ceramic foams are made of silicon carbide, alumina, zirconia, titania, and silica [6,7]. Depending on the cellular structure, the foams are categorized as either open or closed cell foams. In the closed pores there is no or limited connection between the single pores, which might be beneficial for applications requiring high thermal

shock resistance. Therefore, such foams are commonly applied for thermal insulation and fire protection materials, while the open-cell ceramic foams are particularly used for molten metal filtration, diesel engine exhaust filters and hot gas filtration [6,8]. Free space between the ceramic particles allows a large pore volume and a porosity ranging from nanometers to microns or even larger. Subsequently, ceramic foams can be used as membranes, absorbents, in insulation and biomedical devices, as well as catalytic converters [9–11].

Ceramic foam can be produced using various methods, including the replica method [12], starch consolidation [13], the foaming method [14] and gel-casting [11].

The replica method allows an open pore volume of up to 95 % giving an open network of interconnected, but hollow struts. The structure of the resulting foam can be either random or regular depending on the template. Obviously, a large pore volume is accompanied with a low pressure drop and density.

In this work, the replica method was used, which involves coating of the polymer sponge with the ceramic slurry followed by removal of the excess slurry by squeezing, blowing with air to ensure permeability of pores, drying and sintering to remove the polymer components [9]. This procedure results in a ceramic replica of the original polymeric foam. A common challenge in producing porous ceramics with the replica

* Corresponding author.

E-mail address: dmurzin@abo.fi (D.Yu. Murzin).

<https://doi.org/10.1016/j.cattod.2020.09.019>

Received 12 March 2020; Received in revised form 2 June 2020; Accepted 21 September 2020

Available online 30 September 2020

0920-5861/© 2020 Elsevier B.V. All rights reserved.

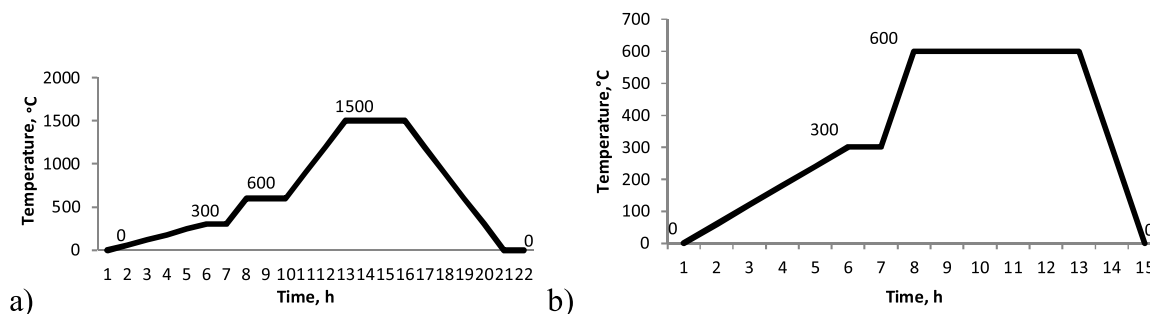


Fig. 1. Heating schedules for calcination of α -alumina support a) per se and b) covered with γ -alumina layer.

method is the choice of a suitable pore size template while retaining an adequate mechanical strength of the final foam. Optimization of different parameters in preparation of the ceramic slurry, subsequent coating of the sponge with the slurry, and sintering is needed to achieve final foams with the desired properties. The sponge used as a replica must be flexible and able to regain its original shape after immersion in the slurry and squeezing. The choice of the polyurethane (PU) sponge pore size and shape is defined by the requirements of the final foam application.

As a carrier material α -alumina was used in the current work, providing required thermal stability. The replica technique was utilized to manufacture a macroporous support by coating the polymer sponge with a ceramic slurry containing α -alumina and a range of additives acting as binders, rheological and anti-foaming agents [15].

The surface area of α -alumina is typically not sufficient to deposit a catalytically active phase, therefore washcoating with γ -alumina was required. Such procedure allows to substantially enhance the surface area from few m^2/g to ca. 250–300 m^2/g [16].

While there are few publications in the literature on catalytic foams development discussing mechanical strength and porosity [17–19] there is a lack of studies addressing the dependence of these parameters on the preparation procedure. The intent of this article is to explore the impact of the preparation procedure on the properties of catalytic foams. The scope of the work is in particular on the investigation of the influence of the number of ceramic layers on strength, porosity and pore interconnectivity of the foams.

Application of ceramic alumina based foams in catalysis has been discussed in the literature [20–22]. In particular, such foams were extensively used in various hydrogenation reactions [23–25].

Hydrogenation of ethyl benzoylformate (EBF) [26] in a continuous up-flow fixed bed reactor was selected as a test reaction in this work. If this reaction is performed with structural catalysts, a catalytically active phase (e.g. Pt) should be introduced on the ceramic foam. To this end the foam was impregnated with an aqueous solution of hexachloroplatinic acid with further treatment resulting in formation of platinum nanoparticles. Pt/ γ -alumina/ α -alumina foams were applied in hydrogenation of EBF in this work to the mixture of mandelates without addition of any optical modifier.

2. Experimental

2.1. Preparation of ceramic foams, washcoating and deposition of the active phase

Two types of commercial PU sponges (15 and 20 PPI where PPI stands for pores per inch) were supplied by Recticel Oy. To remove impurities, PU sponges shaped in a form of a cylinder with defined dimensions (length = 20 mm, diameter = 16 or 20 mm) were cleaned first with distilled water and acetone and thereafter air-blown prior to use. A clean PU sponge was then pretreated to create a sufficient surface roughness for a better suspension adhesion [27] by being placed into 1 M NaOH (Merck, CAS number [1310–73-2]) solution for 24 h, after

which it was dried at 70 °C for 1 h. The samples were washed with water and ethanol and then air-blown followed by two immersions in 30 wt.% silica sol solution (30 wt.%) (Aldrich, 30 wt.%, CAS number [7631–86-9]). After each immersion, the samples were squeezed and blown by air, and dried at 70 °C for two hours. Two immersions were required to adhere a ceramic layer thick enough on the PU surface thus aiding in subsequent coating with α -alumina. As a liquid component of the slurry 5 wt.% PVA (Acros Organics, 5 wt.%, CAS number [9002–89-5]) solution was used.

The slurries were prepared using the following procedure: 9.8 g of α -alumina (Treibcher Schleifmittel/Alodur 220), 0.05 g of titania (Aldrich, CAS number [1317–70-0]) and 0.05 g of magnesia (Fluka, CAS number [1309–48-4]) were mixed with 4.5, 5 or 5.5 mL of PVA solution. The resulting slurries were ground in the ball milling machine (Philips MiniMill) for 45 min.

The coating process included immersion of the sponge in the slurry, air-blowing to remove the excess of slurry and then drying at 70 °C. Immersion was done two to three times. The PU sample might be compressed before the first immersion, therefore it was allowed to expand while being immersed in the slurry. In a typical experimental series, the amount of the liquid phase was increased with every immersion of the PU sample into the slurry in order to keep pore permeability.

Calcination was done in an electrically heated furnace. The coated samples were calcined at 1500 °C for 3 h according to the heating schedule shown in Fig. 1a. Thermal degradation polyurethane foams has been investigated previously in the literature using thermogravimetry [28]. From differential scanning calorimetry the maximum temperature were ca. 315 and 530 °C, thus longer dwelling at two temperatures corresponding to the main degradation stages was applied. The temperature was slowly increased from room temperature to 1500 °C first by heating at a rate 50 °C/h to 300 °C and then to 600 °C with a ramp 5 °C/min. Isothermal conditions were maintained for 1 h at 300 °C and 600 °C in order to burn out the PU matrix. Heating from 600 °C to 1500 °C was done with a ramp with a ramp 5 °C/min. Cooling down from the top firing temperature was slow (5 °C/min) in order to prevent formation of thermal stresses, which could induce cracks in the foam.

Deposition of γ -alumina on the surface of α -alumina carrier was performed in two ways: coating with slurry and deposition from hot water solution of aluminium nitrate.

The slurries were prepared by the following procedure: 5.0 g of γ -alumina was mixed with 8–16 mL of 5% HCl aqueous solution with subsequent ball milling for 30 min.

The coating process was done similarly to the procedure for coating PU sponges with α -alumina. However, no squeezing step was included as the calcined α -alumina foams are not anymore flexible. The sample was immersed once in the slurry, air-blown for removing the excess slurry and dried.

An alternative washcoating process consisted of immersion of α -alumina samples in a aluminium nitrate solution to introduce γ -alumina on the foam surfaces. Two immersions in 1 or 2 M aluminium nitrate solution for 1 min each at 80 °C were performed.

In both cases, calcination was done at 600 °C for 6 h in an electrically heated furnace. The heating schedule is shown in Fig. 1b illustrating that the temperature was slowly increased from room temperature to 600 °C. The same heating protocol was applied as mentioned above (first by heating at a rate 50 °C/h to 300 °C and then to 600 °C with a ramp 5 °C/min). Cooling down was also slow (5 °C/min) in order to avoid any thermal stresses in the foam.

Combination of the two washcoating methods described above by first applying γ -alumina coating from the corresponding suspension followed by deposition from aluminium nitrate was also studied.

Deposition of platinum as the active catalytic component was done using the following procedure: a certain amount of hexachloroplatinic acid (Sigma Aldrich, 241-010-7) (calculated as 5% wt. of γ -alumina in the sample) was dissolved in 600 mL of water. The solution was pumped through the samples of foams by a peristaltic pump (at the speed of 75 mL/min) for 24 h to ensure an efficient deposition of the platinum complex on the foam surface. Deposition of platinum was monitored by a colour change of the solution.

After the deposition, the foam was washed with ammonia (25 wt.%) at room temperature followed by drying at 80 °C. The washed samples were calcined at 400 °C for 3 h. Reduction with flowing hydrogen was performed at 250 °C for 3 h. After reduction the samples were dried at room temperature for 10 h.

2.2. Characterization of the support and the catalysts

The specific surface area and the pore volume were obtained by nitrogen physisorption using Sorptomatic 1900, Carlo Erba Instruments. First the samples were outgassed under vacuum at 150 °C for 3 h and the adsorption/desorption steps were carried at 77 K, using liquid nitrogen as a coolant. The data were interpreted with the Brunauer-Emmett-Teller isotherm and the t-plot methods.

Catalyst images as well as elemental analysis data were obtained with a Leo Gemini 1530 scanning electron microscope (SEM) equipped with a ThermoNORAN + Vantage X-ray detector for energy dispersive X-ray analysis (EDXA) analysis. The images were taken using the secondary electron and backscattered electron detectors at 15 kV, and the in-lens secondary electron detector at 2.70 kV.

The macroporosity of the PU and alumina foams at different preparation steps (i.e. pristine PU, after pretreatment with NaOH, deposition of a silica layer, α -alumina, after washcoating with γ -alumina, as well as after impregnation with hexachloroplatinic acid) was evaluated using an epoxy casting method. About 25 mL of the resin (Elichem Resins Ltd) and 1 mL of the catalyst were mixed and stirred manually for few minutes and then poured in the container until the whole sample was covered. Afterwards, air inside the epoxy resin was removed by a vacuum pump. After drying for 24 h at room temperature, the samples were cut out from the middle and polished to get a smooth surface. Finally, the samples were washed with ultra-pure water and coated with carbon for a better conductivity. SEM images were taken slide by slide and they were attached to each other to make a panorama.

The macroporosity (P) of the foams was calculated using the following equation:

$$P = \frac{\rho_t - \rho_b}{\rho_t} * 100\% \quad (1)$$

where ρ_t is the theoretical density (3980 kg/m³) and ρ_b is the bulk density of the alumina foam.

Compressive strength data of the manufactured carriers was obtained using crush testing. L&W crush tester with two parallel plates (SE 048, Lorentzen & Wettre, Sweden) was used to detect the force needed for an extrudate to collapse. Two plates were moved towards each other using a hydraulic device, recording the pressure at which the catalyst extrudates were broken. The moving speed of the plates was 1 mm/min. The mechanical strength of the foams (20 mm height and 16 mm in

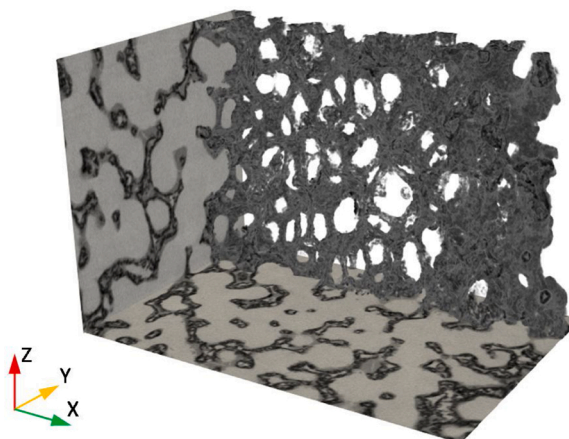


Fig. 2. Exemplary visualisation of measured distributions of local attenuation coefficients using microfocus X-ray CT.

diameter) was determined in the vertical positions.

Transmission electron microscopy (TEM) and X-ray diffraction were applied for catalyst characterization. An energy-filtered transmission electron microscope (EFTEM LEO 912 OMEGA, 120 kV) and a scanning electron microscope (SEM/EDS, Jeol JSM-6400) were used to study the microstructure of the support as well the distribution and the size of the catalyst particles.

The crystal structure of the catalysts was determined by using X-ray diffraction (SiemensD5000 with $CuK\alpha$ radiation).

The three-dimensional (3D) structures of the foams were analysed using a proprietary microfocus cone-beam X-ray computed tomography (μ CT) setup [29] comprising a microfocus X-ray source (XrayWORX XWT-190-TC), a two-dimensional (2D) flat panel X-ray image detector (PerkinElmer XRD 0822 AP3 IND) and a motorized precision rotary stage (FEINMESS DT 105-LM). According to Beer-Lambert's law the intensity measured at each detector pixel gets attenuated by $\exp\left\{-\int \mu(r) dr\right\}$ as the X-ray photons traverse along ray path r through the sample, with $\mu(r)$ being the sample's local linear attenuation coefficient. At an X-ray source voltage of 125 kV sets of one thousand 2D X-ray projection images were acquired while each sample was rotated around 360°. Local attenuation coefficient distributions $\mu(x, y, z)$ are reconstructed from the projection images using a proprietary implementation of the Feldkamp-Davis-Kress algorithm [30,31] onto three-dimensional voxel grids with a resolution of 30 μ m voxel size, as exemplarily shown in Fig. 2. Grey-scale colors represent local attenuation with dark grey corresponding to strong attenuation (i.e. high density) and with light grey corresponding to weak attenuation (i.e. low density). A threshold was applied for the 3D visualisation.

2.3. Catalytic reaction

Hydrogenation of ethyl benzoylformate (EBF) to ethyl mandelate (Fig. 3a) over macroporous Pt/Al₂O₃ catalyst in solvent mixture comprising hexane/2-propanol (90/10) v/v was chosen as a reaction for showing the catalytic activity of the foams. This reaction giving a racemate of R and S mandelate has been previously investigated [26] with the same solvent mixture to facilitate downstream chromatographic separation with a chiral column.

The catalytic activity measurements were performed in an up-flow fixed bed reactor (47 cm length and 3 cm internal diameter) at atmospheric pressure under a flow of molecular H₂ (Fig. 3a).

The testing of the porous catalysts was conducted at 25 °C. To avoid interactions between the catalyst and oxygen, the reaction medium was bubbled with Ar for 10 min before putting it in contact with the catalyst. The liquid phase volume and the initial concentration of EBF were 0.9 L and 5.6 mmol/L respectively. Typically, the experiments were carried

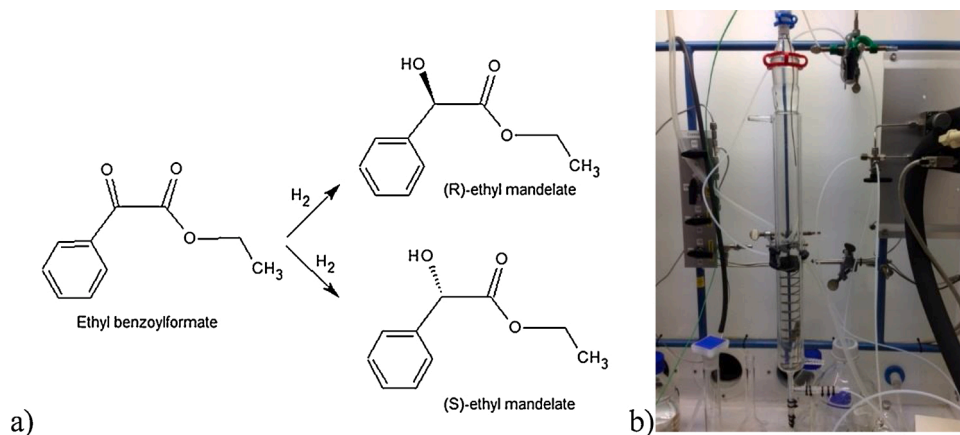


Fig. 3. Reaction scheme for hydrogenation of EBF: a) reaction scheme, b) Up-flow fixed bed reactor.

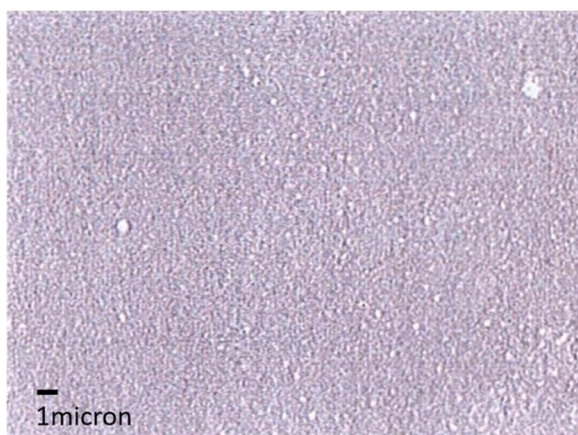


Fig. 4. Surface of PU sponge before pretreatment.

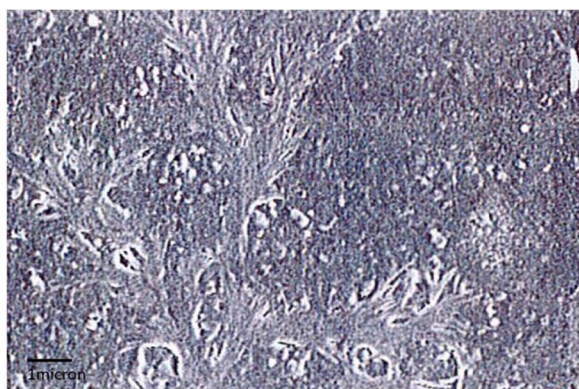


Fig. 5. Surface of PU sponge after etching with NaOH.

out with co-current gas (50 mL/min) and liquid flows (1 mL/min).

The liquid samples were taken periodically and analysed by gas chromatography (GC) using Varian 3300 chromatograph equipped with a chiral column (Silica Chirasil-DEX; length 25 m, diameter 0.25 mm, film thickness 0.25 μm). Helium was applied as a carrier gas with a split ratio of 33. The flame ionization detector (FID) and injector temperatures were 270 and 240 $^{\circ}\text{C}$, respectively. The temperature program of the GC was 120 $^{\circ}\text{C}$ (25 min)–20 $^{\circ}\text{C}/\text{min}$ –190 $^{\circ}\text{C}$ (6 min). The GC analysis was calibrated with ethyl benzoylformate (Aldrich, 95 %, 25,891–1), (R)-ethyl mandelate (Aldrich, 99 %, 30,998–2) and (S)-ethyl mandelate (Aldrich, 99 %, 30,997–4).

3. Results and discussion

3.1. Synthesis of foams

The influence of various processing parameters on properties of porous alumina foams was studied to optimize pore interconnectivity, total porosity and mechanical strength.

One of the most important processes during the ceramic foam preparation is the pretreatment of the PU sponge. The mechanical strength of the foam depends on many parameters and one of them is the attachment of the slurry to the sponge walls. Treatment with 1 M NaOH resulted in cracks on the surface layer of the sponge (Figs. 4 and 5). Based on our preliminary experiments such treatment was needed, otherwise preventing adhesion of the silica layer and eventually formation of stable α -alumina foams.

Etching with NaOH enhances adhesion of the coating to the sponge walls by influencing the sponge surface layers.

Immersing in the silica suspension was done to cover the surface of the polyurethane matrix with a silica layer enhancing the adhesion of the slurry to the PU surface (Fig. 6). Fig. 6 illustrates that immersing in the silica solution results in covering of the surface of the polyurethane matrix with a silica layer.

The slurry for the production of the foams comprised water, grained ceramic powders and an additive. To prepare a slurry with a set of certain properties, it is necessary to change the slurry viscosity, pH or to use different types of additives.

The liquid-to-solid ratio of the slurry plays an important role in the preparation of α -alumina carriers. Slurries with a solid content exceeding 60 % are viscous and cover the surface of PU sponges with thick and irregular layers. As a result, after dipping PU in a slurry, a large part of the cells became blocked. The solid-liquid content was chosen in a way, that the open porosity of the carrier was kept constant connecting the whole foam volume.

Corundum powder with titania and magnesia additives was ground in a planetary mill to decrease the particle size and to improve adhesion parameters. The exact composition is given in the experimental part.

After coating with the slurry, the sponges were dried and sintered. The surface area and porosity of the catalyst based on ceramics depend on the thermal treatment applied during the manufacture. To optimize sintering, it is important to control the heating rate to maximize the final density and minimize the grain growth of the particles.

Alumina can be sintered into ceramic monoliths at temperatures of ca. 1700 $^{\circ}\text{C}$. Sintering at lower temperatures is possible if the grain size is reduced by prolonged milling. Based on the measurements reported in [32], the milling time of 45 min was chosen allowing a decrease of the average particle size from 50 μm to 20 μm which is sufficient for sintering at 1450–1500 $^{\circ}\text{C}$.

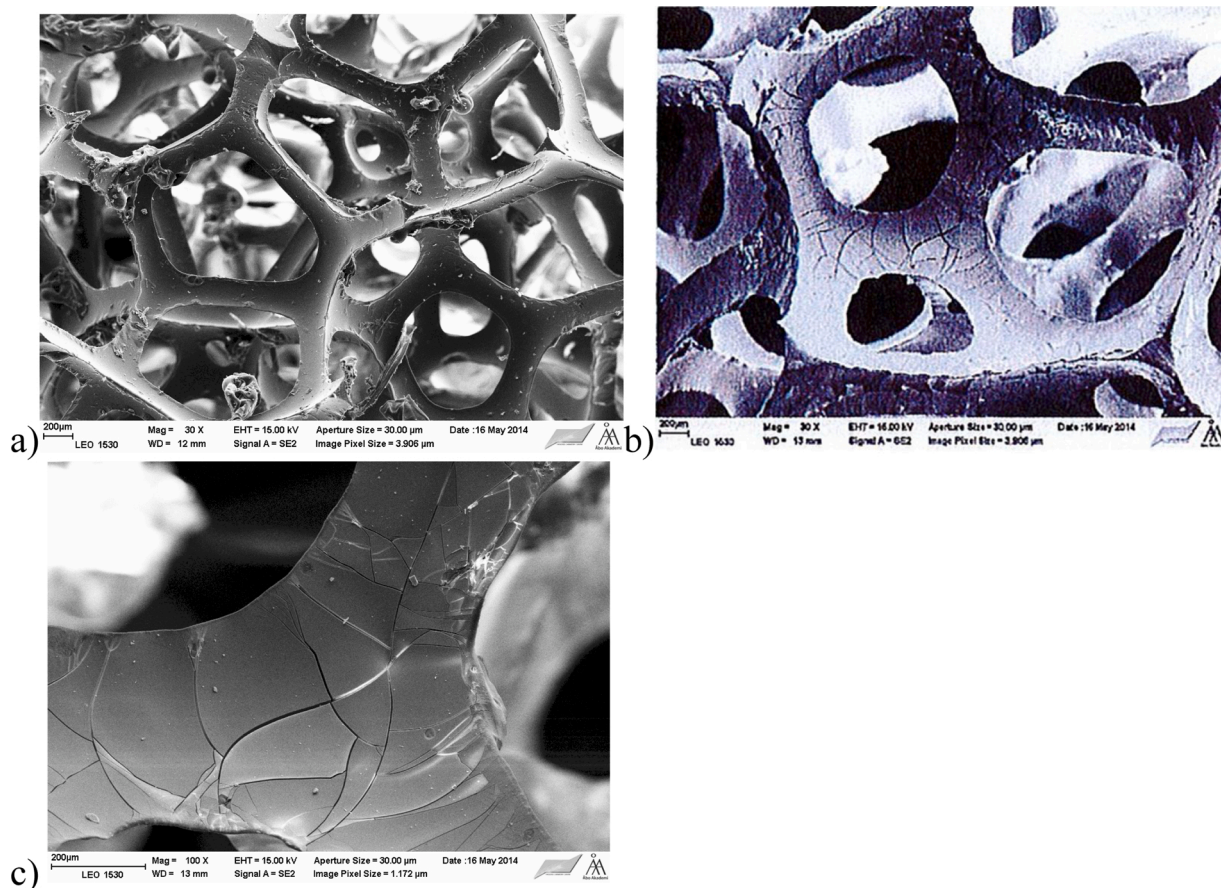


Fig. 6. SEM micrograph of the sponge (ex-20 PU) surface a) prior and after immersing in the silica suspension at different magnification b) 30x, c) 100 × .

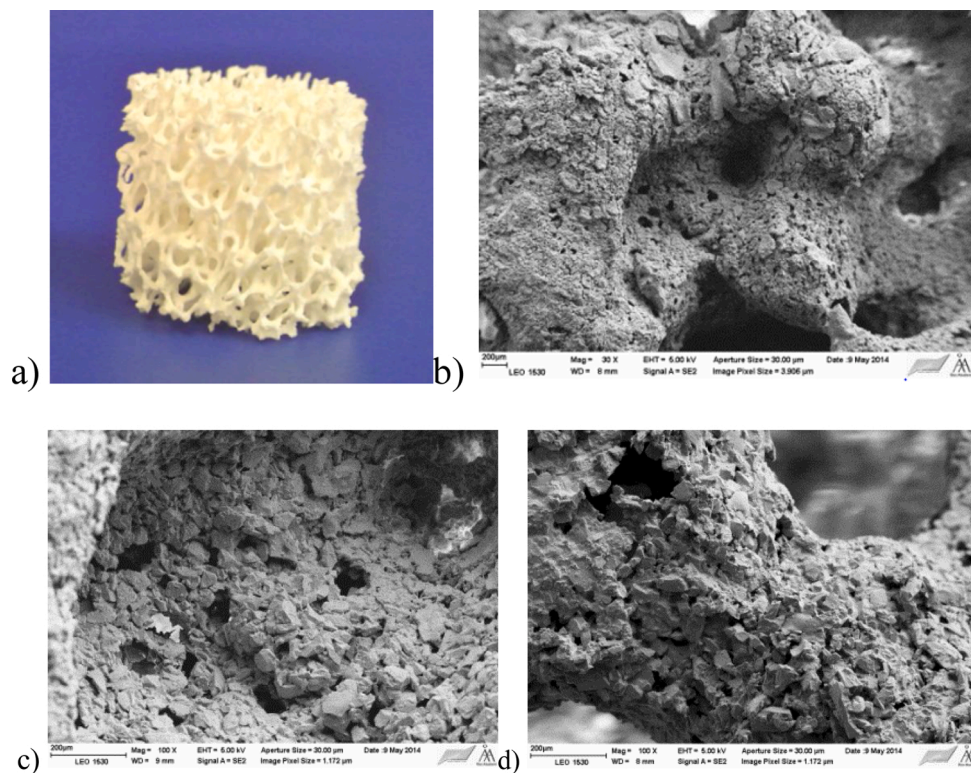


Fig. 7. Images of α -alumina foams, (a); photo; and SEM images of the foam surface b) two dippings with magnesia, $d = 16$ mm, ex-15 PPI, magnification 30 and c) two dippings with magnesia, titania and the antifoam agent, $d = 16$ mm, ex-15 PPI, magnification 100 d) hollow strut of the foam shown in Fig. 7c.

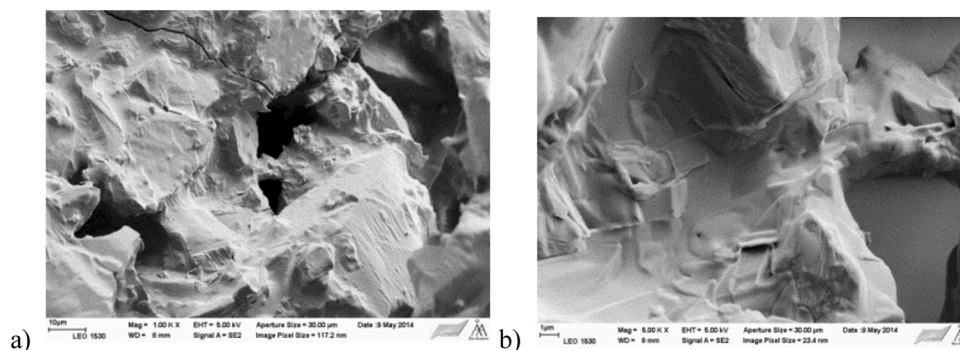


Fig. 8. Surface microstructure of the ceramic foam after sintering (two dippings with magnesia, titania and the antifoam agent, $d = 16$ mm, ex-15 PPI) at different magnification a) 10x and b) 50x.

Fig. 7 displays a photograph of the sintered ceramic foam and SEM images illustrating that the ceramic powder has sintered to give a porous foam with hollow struts.

Immersion of the PU sponge with the slurry was done with the liquid content increasing at every subsequent step: 30–40 % of PVA in the first coating, 50 % in the second and 60–70 % in the third step. With such a procedure, a good pore permeability was achieved with less than 5% of the pores blocked according to visual evaluation. Some of the formed larger round holes are supposed to be generated when gases from the PU sponge matrix were released. Such holes may compromise the mechanical stability of the support.

SEM images of the samples (Fig. 8) show strut surfaces where the particles have partly grown together with sharp particle edges being still visible. Such strut surfaces can accommodate an additional coating layer.

After two or three immersions in the slurry, the samples became capable to endure sintering without collapsing. More experimental work is, however, needed to establish what would be the exact threshold in alumina loading which allows to prevent sintering.

In this work, different ways of sintering and pre-sintering treatments were investigated, with one of them showing a possibility to reduce the amount of the slurry deposited on the PU sponge surface. Pre-sintering at 300 °C for a sufficiently long time was necessary to obtain samples with a required strength, as otherwise materials not exposed to such treatment were not able to withstand sintering without critical structural damages. A need for additional pre-sintering can be explained by diffusion in-between the ceramic slurry and molten polyurethane (at 300 °C), which leads to less damage of the structure of the formed ceramic layer even polyurethane is decomposed caused by a rapid temperature increase [33]. Mechanical properties of such materials, however, could be improved during subsequent coating with α -alumina or washcoating with γ -alumina.

Two additional procedures were involved to increase the surface area by washcoating of the α -alumina foams with γ -alumina.

The first method of increasing the surface area consisted of coating

Table 1

Surface area of foams.

Sample	Foam (wt.% γ -alumina/wt.% α -alumina)	Surface area (BET), m ² /g	Surface area (t-plot), m ² /g
1	γ -alumina (from Al(NO ₃) ₃)/ α -alumina (2/98)	22	48
2	γ -alumina (from suspension)/ α -alumina (5/95)	46	57
3	γ -alumina (from suspension)/ α -alumina (13/87)	61	
4	Pt/ γ -alumina (from suspension)/ α -alumina (0.3/6/93.7)	39	60
5	Pt/ γ -alumina (from suspension)/ α -alumina (0.5/10/89.5)	56	60
6	γ -alumina (combination)/ α -alumina (29/71)	284	
7	α -alumina	Bdl*	

* Below detection limit (no measurable nitrogen adsorption for 0.5 of the foam).

the α -alumina support with an additional layer of γ -alumina utilizing basically the same procedure as for the foam manufacturing via the replica technique. First α -alumina foams were immersed into the slurry with γ -alumina and then calcined in order to attach a layer of γ -alumina on α -alumina carrier. One or two immersions into the slurry were applied. This method allowed to add up to 30 wt.% of γ -alumina (determined by weighing) onto the foam walls. Apparently, washcoating leads to a decrease in the volume of the open pores. Heat treatment at 600 °C was performed after the washcoating.

The second method to increase the surface area of the foams consisted of immersing α -alumina foams or samples coated with γ -alumina suspensions in a hot (75–85 °C) solution of aluminium nitrate, resulting in deposition of γ -alumina. Two immersions for 1 min each were sufficient to increase the mass of the sample by ca. 5 wt.%. Sintering at 600 °C was applied after the washcoating giving the final foam.

SEM images of the foam obtained after washcoating α -alumina

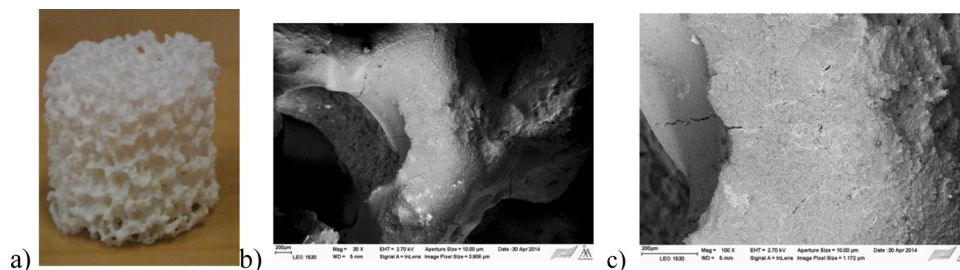


Fig. 9. Sintered γ -alumina/ α -alumina foam prepared by washcoating α -alumina foam using γ -alumina suspension, sintering at 600 °C, washcoating with aluminium nitrate solution and calcination at 600 °C: a) photo and b) SEM image at magnifications b) 30x and c) 100x (three dippings with magnesia, titania and the antifoam agent, $d = 16$ mm, ex-15 PPI).

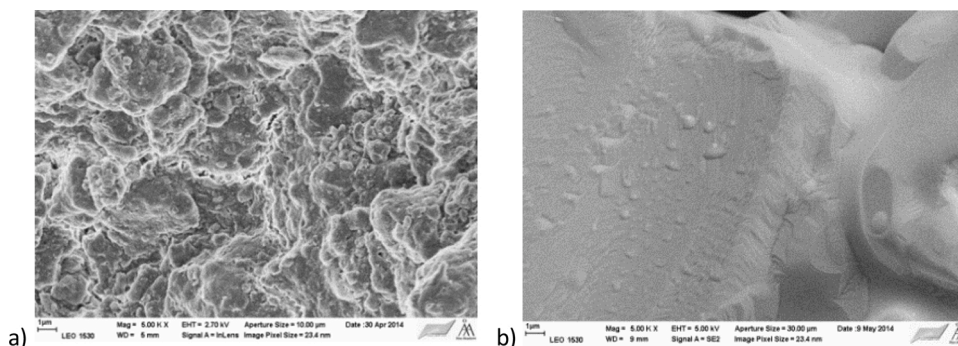


Fig. 10. SEM of a) sintered γ -alumina / α -alumina foam prepared by washcoating α -alumina foam using γ -alumina suspension, sintering at 600 °C, washcoating with aluminium nitrate solution and calcination at 600 °C (three dippings with magnesia, titania and the antifoam agent, $d = 16$ mm, ex-15 PPI) and b) the corresponding α -alumina foam. Both images at magnifications 5kx.

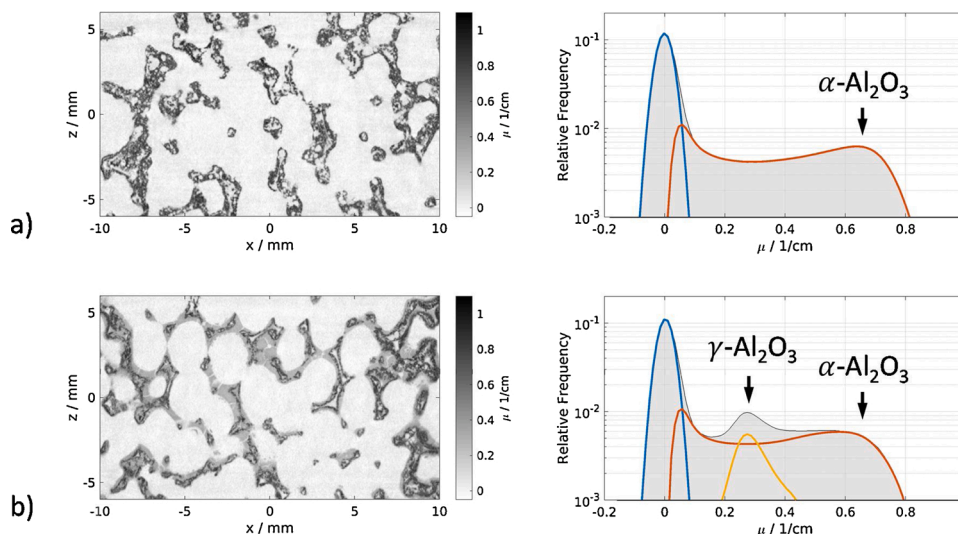


Fig. 11. High resolution X-ray computed tomography of foams, vertical slice images and corresponding histograms of measured attenuation coefficients of a) α - Al_2O_3 and b) γ - Al_2O_3 / α - Al_2O_3 . The histograms (grey shaded) have been empirically decomposed into contributions from void (blue) and ceramic (red and orange) material (For interpretation of the references to colour in this figure legend, the reader is referred to the web version of this article).

support with either aluminum nitrate or γ -alumina (not shown) exhibit morphology to α -alumina support with somewhat less homogeneity of the particles and a minor decrease in dimensions.

As mentioned in the experimental section a combination of the two washcoating methods was also applied meaning that coating with γ -alumina was followed by deposition of aluminium nitrate. The SEM image of such foam is presented in Fig. 9. Physico-chemical properties of the wash-coated foams will be discussed below.

3.2. Physico-chemical and catalytic properties of foams

The surface areas of different foams after washcoating was measured using nitrogen adsorption. The specific surface areas of the materials are summarized in Table 1.

The table reveals that the surface area of the foams after deposition of γ -alumina has increased substantially. Typically, the surface area of α -alumina is 1–5 m^2/g . In the current study the surface area of α -alumina foam was probably even low as it could not be reliably determined from nitrogen physisorption. Such increase as expected was more prominent at a higher washcoating load. Table 1 also illustrates that the combined method, allowing a large amount of washcoat, resulted in a substantial increase of the surface area (compare entries 3 and 6). The deposition of Pt did not markedly influence the surface area (compare entries 3 and 5).

SEM images of the foam obtained by coating α -alumina with γ -alumina and the foam obtained after washcoating the same support with aluminium nitrate and subsequent calcination showed similar morphology. These images (not shown) did not reveal holes that were visible on the surfaces of α -alumina samples.

Surface of the foam prepared with washcoating first the α -alumina foam with γ -alumina suspension and subsequently with aluminium nitrate given in Fig. 10 is shown at a higher magnification than in Fig. 9. In these images the surfaces look much more extended and rough compared to the smooth surface of α -alumina foam taken at the same magnification.

The high resolution X-ray computed tomography of foams (Fig. 11) clearly illustrates that the cross-sections of the foams had decreased after washcoating, because γ - Al_2O_3 fills the pores of the underlying α - Al_2O_3 structure. The greyscale values in the images represent reconstructed X-ray attenuation, which is – for the considered ceramic compound – proportional to their density. For the specific sample presented in Fig. 11b, the density of γ - Al_2O_3 appears to be only 40 % of the density of α - Al_2O_3 , while the overall mass fraction per volume as measured by microfocus X-ray CT increased by factor 1.089 after washcoating.

More quantitative analysis of washcoating was performed by SEM (Fig. 12).

In particular, the SEM images of the cross-section of the foams were used to investigate differences in macroporosity. Fig. 12 shows cross-

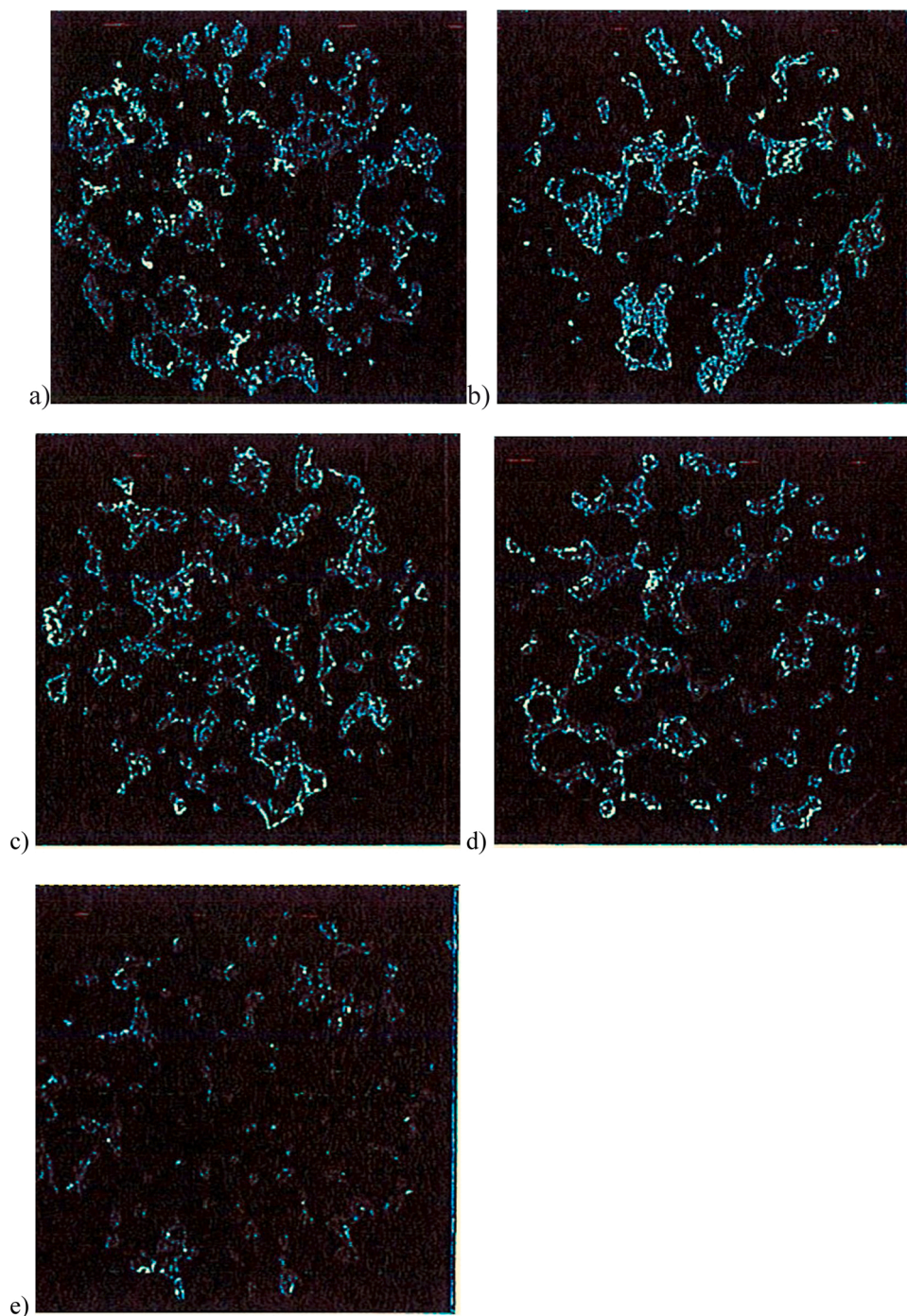


Fig. 12. Cross-sections of foams with increasing number of coating steps from a) 0 to e) 4. In the preparation two dippings with magnesia, titania and an antifoam agent were done, $d = 16$ mm, ex-20 PPI.

Table 2

Crushing strength of foams (16×20 mm) with a different number of coating steps from aluminium nitrate. In the preparation two dippings with magnesia, titania and an antifoam agent were done, $d = 16$ mm, ex-20 PPI.

Number of coating steps	Macroporosity	Weight, g	Maximum pressure, kN	Vertical compression strength, MPa
0	93	1.12	0.17	0.84
1	90	1.51	0.19	0.96
2	87	2.1	0.41	1.31
3	84	3.91	0.57	1.80
4	82	4.46	1.01	3.23

sections of foams, which underwent different number of coatings with γ -alumina. The PU foams used for preparation of ceramic foams had a height of 20 mm being 16 mm in diameter.

Data for the same five α -alumina foams with different content of γ -alumina are shown in Table 2. The first entry corresponds to α -alumina foam without any washcoating. As a comparison, it can be mentioned that a commercial sample of γ -alumina (BDH Ltd) has the compression strength of 19.6 MPa, much exceeding the values for foams. At the same time extrudates [33] made from H-beta zeolite with 30 % bentonite as a binder gave a compression strength of 3–5 MPa depending on the preparation method which is in line with the current results.

Table 2 also illustrates that foams with more coatings had a higher

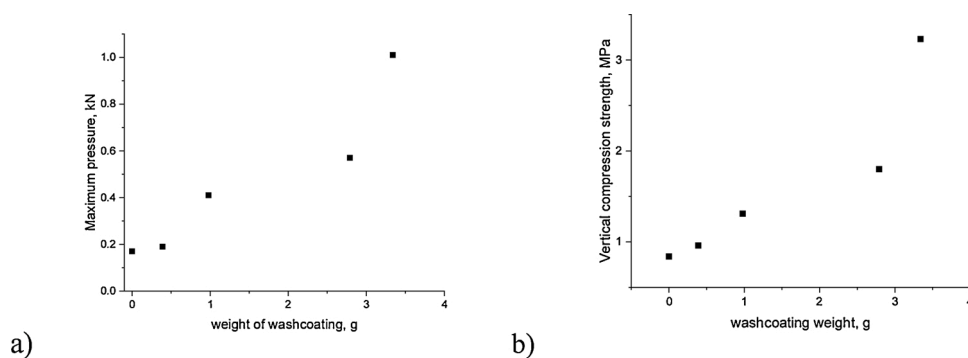


Fig. 13. Dependence of the crushing strength on the washcoating weight in samples with a different number of coating steps, a) maximum pressure, kN, b) vertical compression strength. In the preparation two dippings with magnesia, titania and an antifoam agent were done, $d = 16$ mm, ex-20 PPI.

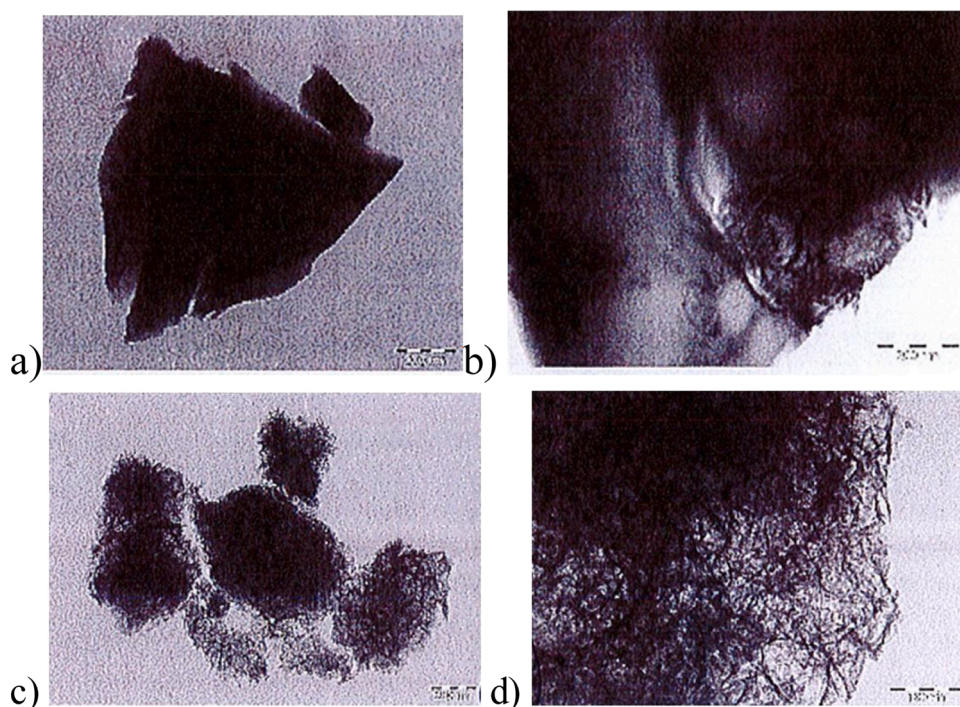


Fig. 14. Images of crushed γ -alumina (from suspension)/ α -alumina: presumably α -alumina (a and b), presumably γ -alumina (c and d).

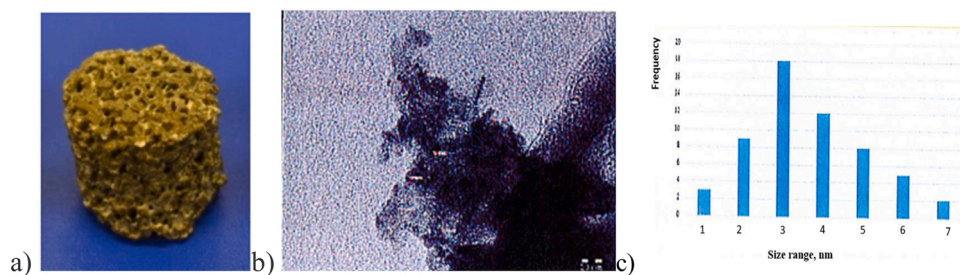


Fig. 15. 5% Pt/ γ - Al_2O_3 / α - Al_2O_3 foam a) photo, b) TEM image of Pt nanoparticles formed after reduction and calcination, c) Pt size distribution.

mechanical strength at the expense of lower pore volume and interconnectivity of the macropores, also visible in Fig. 12. An almost linear dependence of the strength as a function of the solid load can be seen in Fig. 13.

An increase of the mechanical strength of ceramic supports, critical for mechanical durability was previously reported for structured catalysts after washcoating with γ -alumina [34].

TEM images of the crushed γ -alumina (from suspension)/ α -alumina (Fig. 14) underline morphology and crystalline composition of the achieved ceramic material.

Most of the particles have smooth surfaces and sharp edges, while a part of the particles exhibit rough surfaces which can point on α -alumina (Fig. 14 a and b) and γ -alumina (Fig. 14 c and d).

TEM of the catalyst containing 5% Pt/ γ - Al_2O_3 / α - Al_2O_3 (entry 6 in

Table 1) displays (Fig. 15) that the metal is homogeneously distributed across the surface. The average size of Pt clusters was ca. 3 nm. The EDX analysis showed that the metal loading was close to 5 wt% (more precisely 4.96–5.83 depending on the areas in the sample).

For the later catalyst applied in hydrogenation of ethylbenzoyl formate a steady-state was achieved after 2 h. For the liquid sample taken 3.5 h with time-on-stream reactant conversion was 81 % with an overall selectivity to the corresponding alcohols (R-, S-mandelates) equal to 87 %. The rest were by-products in small amounts giving the overall mass balance closure exceeding 95 %.

4. Conclusions

The replica technique was used for preparation of macroporous alumina carriers for catalysis. Pretreatment of the polyurethane (PU) sponge was found to be critical. Treatment with NaOH resulting in cracks on the surface layer of the sponge was found to be essential for stable α -alumina foams formation. A good pore permeability was achieved by immersion of the PU sponge in the suspension several times with increasing polyvinylalcohol content. with less than 5% of the pores blocked according to visual evaluation.

Sintering at 1450–1500 °C into ceramic porous structures was done using pre-milled particles. An efficient way of reduce the amount of the slurry deposited on the PU sponge without structural damage was by pre-sintering at 300 °C for a sufficiently long time.

The surface area of α -alumina foams can be significantly enlarged by coating with γ -alumina using either immersion of α -alumina foams into γ -alumina suspensions followed by calcination or such foams or samples coated with γ -alumina suspensions in a hot (75–85 °C) solution of aluminium nitrate, resulting in deposition of γ -alumina. The latter method was considered to the most promising in terms of the surface area and mechanical stability. Foams with more coatings of γ -alumina had a higher mechanical strength at the expense of lower pore volume and interconnectivity of the macropores. The strength was significantly improved almost linearly when the loading of γ -alumina was increased.

Homogeneous distribution of Pt in the 5% Pt/ γ -Al₂O₃/ α -Al₂O₃ catalyst containing 5 wt.% of Pt with the average size of Pt clusters of ca. 3 nm was achieved using the impregnation method.

Catalytic activity was tested in hydrogenation of ethyl benzoylformate. The catalyst was found to be active demonstrating 87 % selectivity to the desired alcohol products at 81 % conversion of ethyl benzoylformate.

CRediT authorship contribution statement

Vladimir Shumilov: Investigation, Data curation. **Alexey Kirilin:** Investigation. **Anton Tokarev:** Investigation. **Stephan Boden:** Investigation, Data curation. **Markus Schubert:** Investigation, Data curation. **Uwe Hampel:** Methodology, Writing - review & editing. **Leena Hupa:** Project administration, Conceptualization. **Tapio Salmi:** Project administration, Conceptualization. **Dmitry Yu. Murzin:** Supervision, Conceptualization, Writing - original draft, Writing - review & editing.

Declaration of Competing Interest

The authors declare that they have no known competing financial interests or personal relationships that could have appeared to influence

the work reported in this paper.

Acknowledgement

The authors are grateful to Linus Silvander for SEM analysis. Financial support from the Graduate School in Chemical Engineering (GSCE) to Vladimir Shumilov and Academy of Finland to Tapio Salmi is gratefully acknowledged.

References

- [1] C.P. Stemmet, Gas-liquid Solid Foam Reactors: Hydrodynamics and Mass Transfer, PhD Thesis, Technical University of Eindhoven, 2008, <https://doi.org/10.6100/IR635735>.
- [2] M. Saber, T.T. Huu, C. Pham-Huu, D. Edouard, Chem. Eng. J. 185-186 (2012) 294–299.
- [3] V. Blachou, D. Goula, C. Philippopoulos, Ind. Eng. Chem. Res. 31 (1992) 364–369.
- [4] Y.S. Han, J.B. Li, Y.J. Chen, Q.M. Wei, J. Mater. Proc. Tech. 128 (2002) 313–317.
- [5] J. Luyten, S. Mullens, J. Coymans, A.M. De Wilde, I. Thijs, R. Kemps, J. Eur. Ceram. Soc. 29 (2009) 829–832.
- [6] S. Sharafat, N. Ghoniem, M. Sawan, A. Ying, B. Williams, J. Am. Ceram. Soc. 81 (2006) 455–460.
- [7] S. Dhara, P. Bhagarva, J. Am. Ceram. Soc. 86 (2003) 1645–1650.
- [8] H.X. Peng, Z. Fan, J.R.G. Evans, J.J.C. Busfield, J. Eur. Ceram. Soc. 20 (2000) 807–813.
- [9] J. Saggio-Woyansky, C.E. Scott, W.P. Minnear, Am. Ceram. Soc. Bull. 71 (1999) 1674–1682.
- [10] X. Zhu, D. Jiang, S. Tan, Mater. Res. Bull. 37 (2002) 541–553.
- [11] P. Sepulveda, Ceram. Bull. 76 (1997) 61–65.
- [12] H. Schmidt, D. Koch, G. Grathwohl, P. Colombo, J. Am. Ceram. Soc. 84 (2001) 2252–2255.
- [13] O. Lyckfeldt, J.M.F. Ferreira, J. Eur. Ceram. Soc. 18 (1998) 131–140.
- [14] W.P. Minnear, Processing of foamed ceramics, in: M.J. Cima (Ed.), Ceramic Transactions, Forming Science and Technology for Ceramics, Am. Ceram. Soc., Westerville, OH, 1992, pp. 149–156.
- [15] K. Ishizaki, S. Komarneni, Porous Materials: Process Technology and Applications, Klumer Academic Publishers, London U.K, 1998.
- [16] M.V. Twigg, J.T. Richardson, Ind. Eng. Chem. Res. 46 (2007) 4166–4177.
- [17] B. Simon, M. Seeber, U.T. Gonzenbach, L.J. Gauckler, J. Mater. Res. 28 (2013) 2281–2287.
- [18] A. Manonukul, P. Srikudvien, M. Tange, C. Puncre, Mater. Sci. Eng. A. 655 (2016) 388–395.
- [19] L. Samain, A. Jaworski, M. Eden, D.M. Ladd, D.-K. Seo, F.J. Garcia-Garcia, U. Hausermann, J. Solid. St. Chem. 217 (2014) 1–8.
- [20] E. Behraves, L. Hupa, T. Salmi, D.Yu. Murzin, Catal.-Spec. Period. Rep., Royal Soc. Chem. 28 (2016) 28–50.
- [21] M. Twigg, J.T. Richardson, Stud.Surf. Sci. Catalysis 162 (2006) 135–142.
- [22] R. Faure, F. Rossignol, T. Chartier, C. Bonhomme, A.S. Maitre, G. Etchegoyen, P. Del Gallo, D. Gary, J. Europ. Ceram. Soc. 31 (2011) 303–312.
- [23] V.N. Grunskii, M.G. Davidkhanova, M.D. Gasparyan, S.E. Zolotukhin, Fibre Chem. 51 (2019) 240–243.
- [24] O.V. Starodubtseva, V.N. Grunskii, A.V. Bespalov, G.V. Avramenko, A.V. Ignatov, Yu.A. Pinchuk, Khimich. Tekhnol. (Moscow) 14 (2013) 599–605.
- [25] A.V. Ignatov, A.E. Varakutin, I.N. Solov'eva, I.B. Karmanova, I.A. Kozlov, M. N. Semenova, V.V. Semenov, Russ.Chem. Bull. 67 (2018) 1394–1400.
- [26] G. Martin, P. Maki-Arvela, D.Yu. Murzin, T. Salmi, Top. Catal. 57 (2013) 1576–1581.
- [27] H.E. Bergna, W.O. Roberts, Colloidal Silica: Fundamentals and Applications, CRC Press, Baton Rouge, 2005.
- [28] L. Jiao, H. Xiao, Q. Wang, J. Sun, Polym. Degrad. Stab. 98 (2013) 2687–2696.
- [29] S. Boden, M. Bieberle, G. Weickert, U. Hampel, Powder Techn. 188 (2008) 81–88.
- [30] L.A. Feldkamp, L.C. Davis, J.W. Kress, J. Opt. Soc. Amer. A 1 (1984) (1984) 612–619.
- [31] A.C. Kak, M. Slaney, Principles of Computerized Tomographic Imaging, IEEE Press, New York, 1987. ISBN:0-87942-198-3.
- [32] T. Fey, U. Betke, S. Rannabauer, M. Scheffler, Adv. Eng. Mat. 19 (2017), 1700369.
- [33] Z. Vajglova, N. Kumar, M. Peurla, L. Hupa, K. Semikin, D. Sladkovskiy, D. Yu. Murzin, Ind. Eng. Chem. Res. 58 (2019) 10875–10885.
- [34] A. Cybulski, J.A. Moulijn, Structured Catalysts and Reactors, CRC Press, Boca Raton, FL, 2005.